

MAGNETIC SUSPENSION OF THE ROTOR OF AN ARTIFICIAL HEART - IMPROVEMENTS TO THE RADIAL STIFFNESS

Fernando A. Camargo, fernando.antonio@poli.usp.br
Oswaldo Horikawa, oswaldo.horikawa@poli.usp.br
Department of Mechatronics Eng., Escola Politécnica of São Paulo University

Isaias da Silva, isaias.silva@unifesp.br
Department of Natural sciences, Federal University of São Paulo

Aron J. P. Andrade, aron@dantepazzanese.org.br
Dante Pazzanese Cardiology Institute

Pedro I. T. C. Antunes, antunes.pedro@usp.br
Department of Mechatronics Eng., Escola Politécnica of São Paulo University

Eduardo G. P. Bock, ebock@dantepazzanese.org.br
Dante Pazzanese Cardiology Institute

Abstract. – *This report presents some improvements to the radial stiffness of a magnetic suspension in a new ventricular assist device (VAD) that has been jointly developed by Dante Pazzanese Cardiology Institute (IDPC) and Escola Politecnica of São Paulo University. This VAD has a novel architecture that distinguishes it from other known VADs. In this, the rotor that impels and pressurizes the blood has a conical geometry with spiral impellers. Whereas, in the first VAD models, the rotor was held by ball bearings. One of the objectives of this project is to develop a VAD that uses a magnetic bearing to bear the rotor. The magnetic suspension minimizes hemolysis and improves VAD lifetime, thanks to the absence of any contact between pump rotor and body. A hybrid type magnetic bearing that combines permanent magnets with electromagnets and executes active control in only axial direction of the rotor is used. This magnetic bearing suspension architecture is simpler and less expensive than those that use active control in two or more degrees of freedom in a rotor and also has low energy consumption and heat dissipation, because the control of each degree of freedom requires a sensor, an electromagnetic actuator, an amplifier and a controller. However, the absence of active control along radial directions can be a source of problems, unless a higher radial magnetic passive stiffness is assured. So, after presenting in a past work, the design procedure of the magnetic bearing, the first prototype has been constructed. In addition to presenting the prototype, this report also describes the problems of poor radial stiffness in it and a way of achieving a higher level of radial stiffness. In this sense, different types of electromagnetic actuators are proposed and the action of each actuator studied by numerical methods and by experiments.*

Keywords: Ventricular assist device, Rotary blood pump, Mixed flow blood pump, Magnetic bearing system.

1. INTRODUCTION

Lately, the researches aiming the development and also the enhancement of new ventricular assist devices (VADs) have increased, this is due to the higher demand of such devices for patients that suffer from chronic cardiovascular diseases and that have to wait a long time for heart transplantation or are not eligible for organs transplant, Hoshi *et al.* (2005). Other important reasons to develop VADs are:

- Small availability of donors;
- Low infection risk delivered;
- Low behavioral restriction;
- The benefit brought when they are put to work together with the debilitated natural heart because they can help recovery, acting in this case as regenerative medicine.

So, in this context, this report has as fundamental object, that is to study a ventricular assist device previously developed by Dante Pazzanese Cardiology Institute (VAD-IDPC), (Andrade *et al.* 1996). This VAD (Fig. 1) has a novel architecture that distinguishes it from other known VADs. Here, the rotor that impels and pressurizes the blood has a

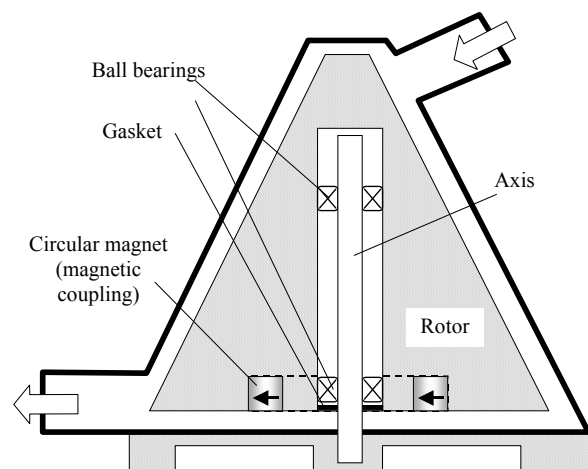


Figure 1. VAD-IDPC scheme.

conical geometry with spiral impellers, not shown in Fig. 1. Other known VADs can be classified in two main categories, those that use centrifugal pump principle and the others based on axial pump principle. Examples of radial VADs are VentrAssist (Esmore *et al.* 2005), Duraheart (Nojiri, 2002) and CorAide (Fukumachi *et al.* 2002) among others, while examples of axial VADs are Hemopump (Don, 2000), Jarvik2000 (Westby *et al.* 1998) and Micromed DeBakey (Wieselthaler *et al.* 2000) among others. Commonly, radial pumps give larger liquid heads, when compared to the axial ones, that is, larger liquid pressure difference between pump input and output. In contrast, axial pumps give larger flow rate, contributing to reduced pump size. Thus, when radial and axial pumps are used as VADs, assuming same flow rate and liquid head for both models, the first operates with lower rotation in the rotor, but they have larger dimensions. It is equivalent to say that axial VADs make possible a more compact VAD but they demand a higher speed in the rotor.

Thereby, both types of VADs present potential advantages and disadvantages. The reduced size is very interesting for the development of implantable VADs. However, low rotor operational speed is interesting to minimize the risk of the hemolysis, that is, the harm of blood cells by collisions with the rotor at a high speed and also by shear stress. Moreover, low rotor speed contributes to simplify the control and the driving of the rotor. In this scenario, VAD-IDPC presents an intermediate solution, e.g. it can operate in rotations about 80% lower than that of axial pumps and its conical rotor has an average diameter of approximately half of the radial pump types. Nevertheless, the first built VAD-IDPC prototype used mechanically sealed ball bearing to support the rotor, see Fig. 1. So, this kind of bearing has some drawbacks, i.e., the blood can pass through the seals reaching the bearing balls and its lubricant causing blood contamination, blood hemolysis and locking the bearings. Therefore, the replacement of ball bearings suspension for magnetic bearings suspension can improve VAD life time, contributing to reduce hemolysis level and improving VAD reliability. Thereby, a hybrid type magnetic bearing that uses control in a single direction of a rotor and that works in attraction mode is used to support VAD-IDPC rotor, (Silva and Horikawa, 2000). However, such magnetic bearing suspension architecture has some drawbacks, like constant stiffness along two radial and two angular passive directions that can cause rotor instability when it passes through critical speeds and also due to some unbalancing forces. So, in order to improve this passive radial and angular stiffness a magnetic suspension that uses high performance permanent magnets, such as rare earth magnets, is required. The bearing hybrid electromagnetic actuator types must also be well designed so that they keep a small size and can assure rotor axial stable equilibrium under several rotor speed ranges and the power dissipation through the coils must be small, thus reducing the energy spent. So, in this context, this report presents some theoretical and experimental preliminary results of magnetic force and stiffness obtained by finite element analysis and by experiments conducted on different electromagnetic actuator designs and also in a VAD simplified prototype.

2. ELECTROMAGNETIC ACTUATORS - NUMERICAL AND EXPERIMENTAL ANALYSIS

Firstly, three open magnetic circuit electromagnetic actuator architectures were analyzed by numerical methods and also experimentally. The whole electromagnetic design has equal dimensions and number of coil turns, Fig. 2. The main difference between them is the material of its core, one made entirely of iron, another using a cylindrical shape NdFeB permanent magnet and the third core composed of iron and NdFeB cylindrical permanent magnet, Figs. 2(a), (b) and (c). The number of coil turns is 450 and

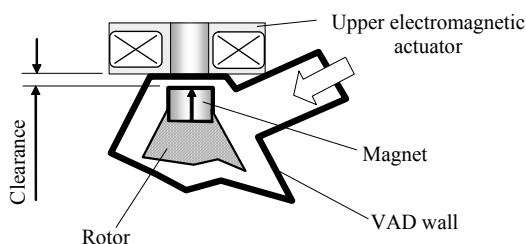


Figure 3. VAD upper part detail.

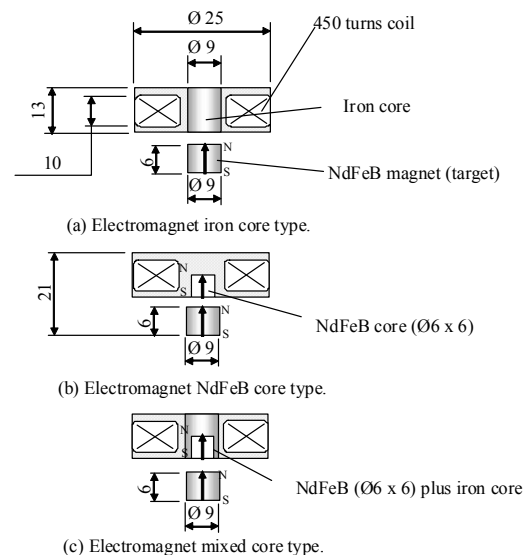


Figure 2. Three upper electromagnetic actuators architectures analyzed.

was determined based only on actuator limiting dimensions. A cylindrical shape NdFeB magnet was chosen as target and the clearance between actuator and the target is 2mm, Fig. 3. This 2mm clearance allows a VAD with a wall thickness of at least 1mm and other 1mm free

space for blood flowing through the rotor and the VAD body, Fig. 3. As mentioned, the actuators shown in Fig. 2 have an opened magnetic circuit and this configuration was chosen because it can provide its dealers with both electromagnetic attraction and repulsion forces due to the magnetic interaction between magnetic fields produced by actuator and by the target permanent magnet. This is important in the sense of simplifying the control system, e.g. it is possible the use of only one power amplifier thus reducing VAD energy consumption and also its final cost. The three magnetic actuators shown in Fig. 2 are the upper VAD magnetic bearing actuator. The lower VAD actuator architecture is analyzed sequentially.

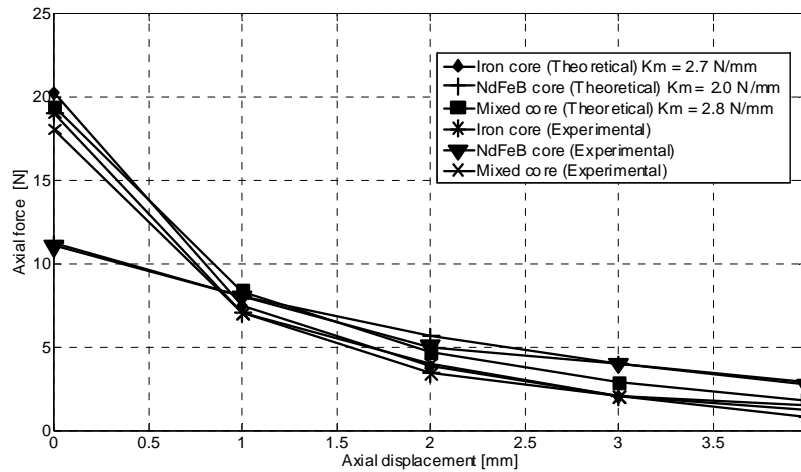


Figure 4. Magnetic axial forces as function of target permanent magnet axial displacement for null current through the coils (Upper actuator).

Figure 4 shows the numerical and experimental results of magnetic axial forces as a function of target magnet axial displacement for the actuators depicted in Fig. 2 and without any electric current applied to the coils. The numerical analyses were made using a finite element electromagnetic simulation software package and the experimental results measured using a mechanic setup. Through Fig. 4 one can see that the experimental and theoretical results have a reasonable approximation and considering an axial displacement ranging from 1 to 3mm the utmost magnetic constant K_m value occurs for the mixed core actuator type, Fig. 2c. This is because of the high magnetic flux density due to the NdFeB magnet together with the iron contribution delivered to the gap region that improves the magnetic attraction force. The maximum theoretical magnetic flux density values observed in the gap region were 1, 1.15 and 1.46 Tesla for the iron core, NdFeB core and mixed core actuators, respectively.

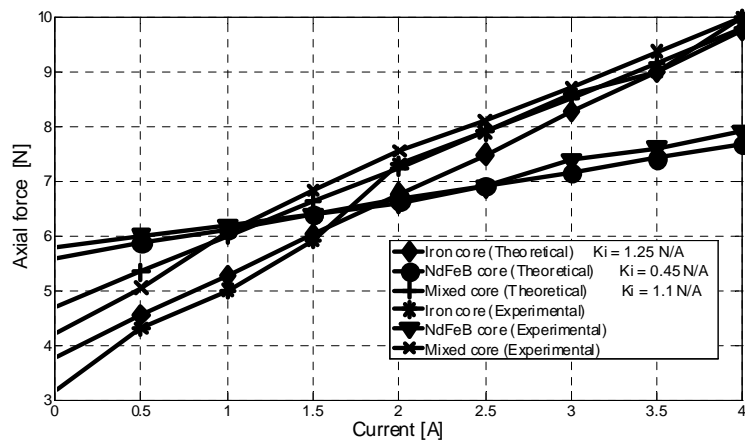


Figure 5. Magnetic axial forces as a function of current for 2mm gap (Upper actuator).

Figure 5 depicts the magnetic axial forces for upper actuator configurations as a function of electrical current and when the gap between the actuator core and the target permanent magnet measures 2mm and

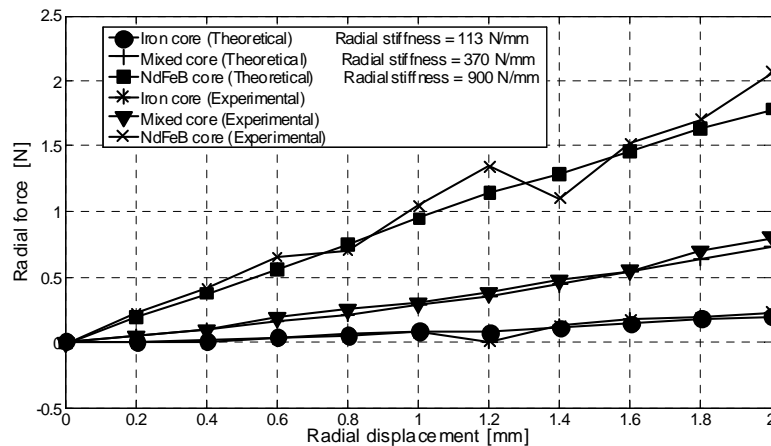


Figure 6. Magnetic radial forces as function of target permanent magnet radial displacement for 2mm gap (Upper actuator).

remains constant. This figure shows that the maximum electromagnetic constant K_i value is 1,25 N/A and occurs for the actuator using iron core. This is explained by the higher iron magnetic permeability in comparison with the lower permeability of the NdFeB magnet.

Figure 6 presents the radial magnetic forces for the upper actuator designs and as function of the target magnet radial displacement relatively to actuator center position. Observing Fig. 6 one can see the electromagnetic actuator having a NdFeB magnet core, as shown in Fig 2b, delivering the greatest radial stiffness intensity among the three analyzed configurations. According to Yonnet, 1982, when two cylindrical shape permanent magnets, operating in attraction mode and without iron working together, the magnetic radial stiffness value is exactly half of the axial stiffness value. This result is because of the high dispersal magnetic field surrounding the magnets.

The VAD architecture proposed here uses an inductive cylindrical shape sensor type located in its lower side to control rotor axial displacements. So, the use of such sensor do not allow for the VAD's lower side the same actuator design as used for its upper side, as depicted in Fig.2. Therefore new lower actuator architecture has been proposed and analyzed by numerical methods and experimentally. This VAD's lower actuator is shown in Fig. 7 and it has a FeBa circular ring shape magnet fixed at the actuator, a 450-turn coil and a NdFeB circular ring magnet as a target. The numbers of coil turns and the magnet dimensions have been chosen based only in VAD limit dimensions.

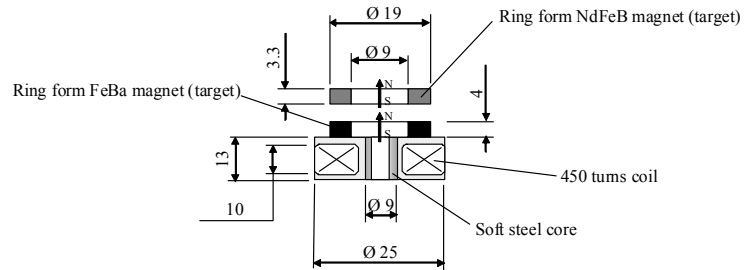


Figure 7. VAD lower electromagnetic actuator analyzed architecture. The numbers of coil turns and the magnet

Figures 8, 9 and 10 show the lower actuator theoretical and experimental magnetic force results as a function of the target axial displacements of the electric current through the coil and of target radial displacements relative to actuator central position for a 2mm gap, respectively. Comparing the results depicted by Figs 8, 9 and 10 with those shown by Figs 4, 5 and 6 one can observe that the three upper actuator architectures presented in Figs 2 have better performances than the lower actuator design. These lower actuator deficiencies are mainly due to the use of the FeBa magnet that has poorer remanent induction than that of the NdFeB magnets. Despite of this poor lower actuator performance, the use of FeBa magnet working together the NdFeB magnet is necessary, because it was observed during the simulations that the use of two NdFeB magnet rings, although improving both actuator axial force and radial stiffness, the actuator electromagnetic force as a function of current was not capable of keeping the rotor working with a clearance of 2mm.

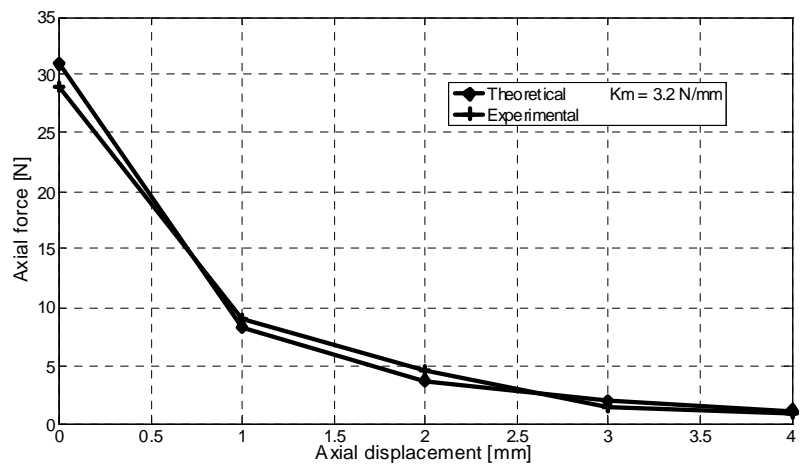


Figure 8. Magnetic axial forces as a function of target permanent magnet axial displacement for null current through the coils (Lower actuator).

The results shown in Figs 4, 5, 6, 8, 9 and 10 are in some aspects conflicting. As previously mentioned, in one degree of freedom controlled magnetic bearing the passive stiffness must be improved, which means the use of an actuator type depicted in Fig 2b and that assures, together the lower actuator, a VAD rotor radial stiffness of

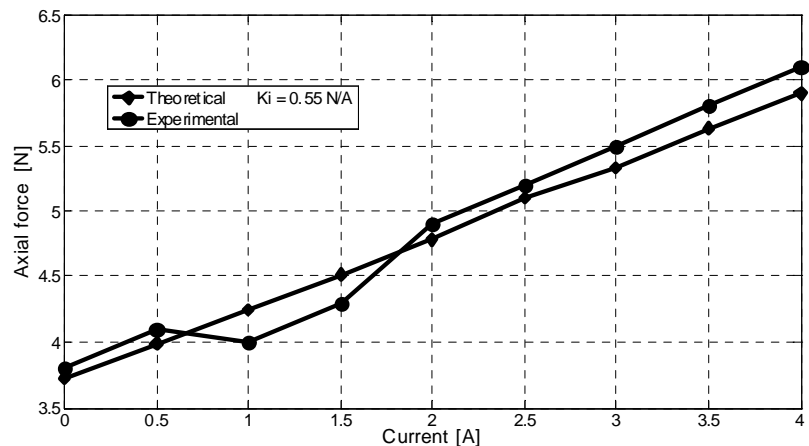


Figure 9. Magnetic axial forces as a function of current for 2mm gap (Lower actuator).

approximately 1000 N/mm, see Figs 6 and 10. On the other hand, the actuator architecture shown in Fig. 2b has the poorest electromagnetic constant K_i value among the three actuator configurations, and this implies an actuator with lower electromagnetic efficiency, i.e. it requires high current densities to assure an electromagnetic force capable of keeping the VAD rotor in a stable axial position, and this fact must be avoided for VADs in general, because it will cause the blood temperature elevation, higher energy consumption among other non-desirable drawbacks. So, regarding the three proposed upper actuator architectures plus the suggested lower actuator design, the actuator presented by Fig. 2c is the best choice for using in the VAD magnetic suspension described and analyzed herein.

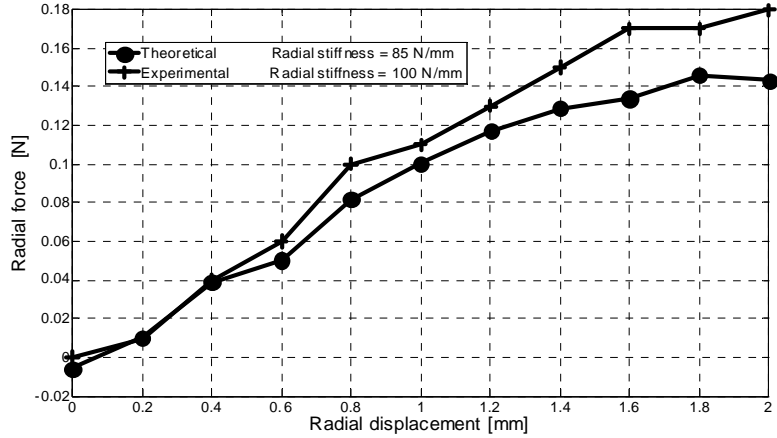


Figure 10. Magnetic radial forces as function of target permanent magnet radial displacement for 2mm gap (Lower actuator).

3. MAGNETIC SUSPENSION FOR VAD-IDPC SCHEME

Figure 11 shows the VAD-IDPC scheme with the proposed magnetic suspension. The VAD upper and lower actuators are those presented in Figs. 2c and 3, and they were chosen based on the preceding actuator analyzes. The VAD rotor has a conical shape and two magnets are fixed on its end, i.e. a cylindrical shape NdFeB magnet is fixed on the upper end and a ring shape FeBa magnet is fixed on its lower end and it is positioned between the upper and the lower actuators. As the magnets fixed to the rotor and the actuator magnets work in attraction mode, the rotor has stable passive radial stability. So, assuring a minimal length to the rotor, i.e. rotor length twice as higher than the rotor fixed magnet diameter, the angular rotor passive stability is also assured (Silva and Horikawa, 2000). Thus the only unstable rotor degree of freedom is its axial direction, and in order to stabilize this rotor direction, a control system composed of a non-contacting tubular inductive type sensor, a controller and a power amplifier is used.

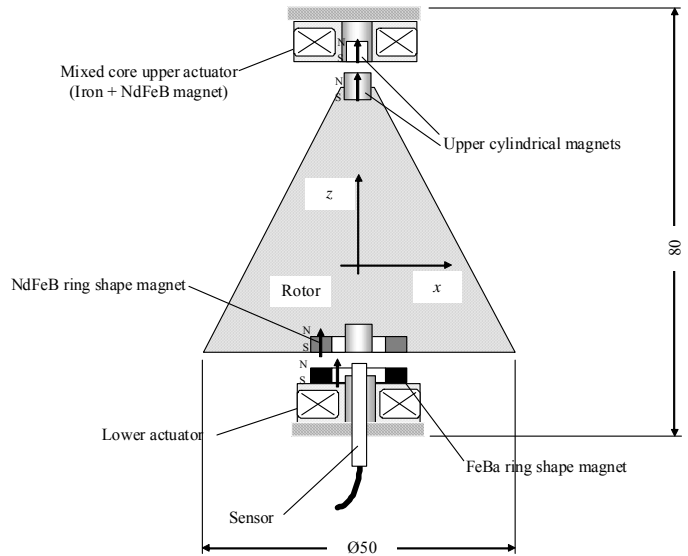


Figure 11. VAD-IDPC scheme using magnetic suspension with active control only along axial (z) direction.

4. MODELING AND CONTROLLING THE MAGNETIC SUSPENSION FOR VAD-IDPC

The VAD magnetic bearing axial direction suspension control system is modeled assuming some simplifications:

- the rotor remains symmetric about the x, y and z-axes;
- the displacements are small and occur about the rotor axial equilibrium position and
- the magnetic attraction force and the electromagnetic force in the axial direction can be linearized with respect to the nominal operating point of equilibrium (i_0, z_0) .

The VAD controlled axial direction dynamic model is shown in Fig. 12. As depicted in this figure equals current flow through both electromagnetic coils, thus, the electromagnetic attraction and repulsion forces are obtained by mounting the coils by reversed polarity in each actuator side. The magnetic force $f_m(t)$ and the electromagnetic term $f_{em}(t)$ have been linearized according to the axial displacement $\Delta z(t)$ and to the electric current $\Delta i(t)$ as follows:

$$f_m(t) = k_m \Delta z(t) \quad (1)$$

$$f_{em}(t) = k_i \Delta i(t)$$

Where, in Eqs. 1 and 2, t is the time; k_m and k_i are the magnetic and the electromagnetic constants, respectively. The electromagnetic constant k_i , in Eq. 2, is function of nominal displacement z_o . On the other hand, considering the use of electromagnets with both constant inductance L and resistance R , the dynamic behavior of the electromagnetic coil is given by the following equation:

$$L \frac{d\Delta i(t)}{dt} + R\Delta i(t) = v(t) \quad (3)$$

Using Eqs. 1 ~ 3 the open loop VAD's rotor axial direction magnetic suspension transfer function $G(s)$ is obtained:

$$G(s) = \frac{\Delta Z(s)}{\Delta V(s)} = \frac{k_i}{Lm} \cdot \frac{1}{s^3 + \frac{R}{L}s^2 + \frac{k_m}{m}s + \frac{Rk_m}{Lm}} \quad (4)$$

Here, z and m are the gap deviation from nominal operation point (VAD rotor axial direction) and the mass of the rotor, including the rotor magnets, respectively. In this system only one gap sensor is used, and the measured variable was the z axial position. The system described by Eq. 4 is stabilized by an ordinary PID (Proportional – Integral – Derivative) type controller given by:

$$G_c(s) = k \left(1 + \frac{1}{T_i s} + \frac{T_d s}{\tau s + 1} \right) \quad (5)$$

Where k is the proportional gain of the controller, T_i is the time constant of the integral element and T_d is the time constant of the derivative element. Each controller term has a specific effect on the VAD's rotor magnetic bearing suspension behavior, i.e., the proportional term makes the current changes proportional to the size of the error signal. This results in bearing behavior analogies to a spring. The rotor force returning to the center position of the bearing increases by a direct relationship with the error signal of the rotor axial position. Therefore, a bearing system with a simple proportional control will oscillate and become unstable because there is no mechanism to provide damping effect for the system. The required damping can be introduced using a derivative control. The derivative control produces a force that is proportional to the velocity of the rotor axial position.

This results in a bearing removing energy from the VAD rotor. Actually, the derivative control works as a shock absorber. However, a controller with only proportional and derivative terms will always have a steady state offset from the set point. This is due to the fact that the proportional and derivative controllers only deliver a non-zero output if there is a position error. In order to solve this position error an integrator is used. The integrator produces output that increases at a rate that is proportional to the size of the error signal over time. Thus, the longer non-zero error signal is, the larger the integrator output gets. The integrator will hold its output constant if no error signal is presented. For steady state conditions, the integrator increases the output until the error signal is zero (Aström and Hägglund, 1988). The block diagram of the control system for VAD rotor axial direction is depicted in Fig. 13.

Where k is the proportional gain of the controller, T_i is the time constant of the integral element and T_d is the time constant of the derivative element. Each controller term has a specific effect on the VAD's rotor magnetic bearing suspension behavior, i.e., the proportional term makes the current changes proportional to the size of the error signal. This results in bearing behavior analogies to a spring. The rotor force returning to the center position of the bearing increases by a direct relationship with the error signal of the rotor axial position. Therefore, a bearing system with a simple proportional control will oscillate and become unstable because there is no mechanism to provide damping effect for the system. The required damping can be introduced using a derivative control. The derivative control produces a force that is proportional to the velocity of the rotor axial position.

5. MAGNETIC SUSPENSION PROTOTYPE FOR VAD-IDPC

Based on considerations presented above, about the most excellent actuator scheme to be used in the proposed VAD-IDPC magnetic bearing suspension, a prototype of the bearing was developed and tested. Figure 14 shows the

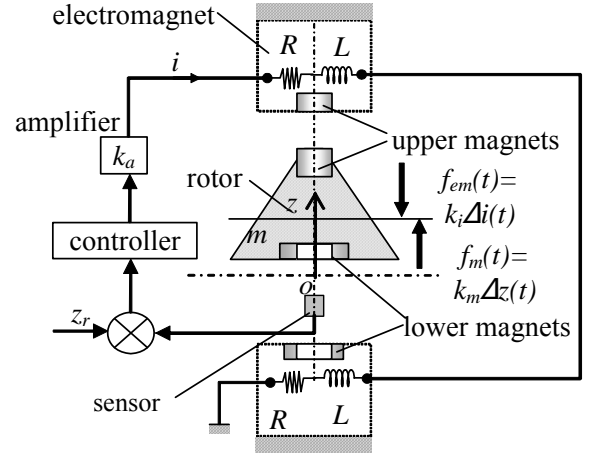


Figure 12. VAD magnetic suspension dynamic model.

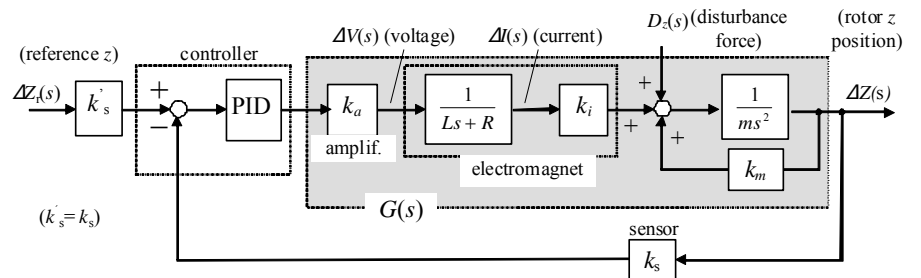


Figure 13. VAD magnetic suspension control system block diagram.

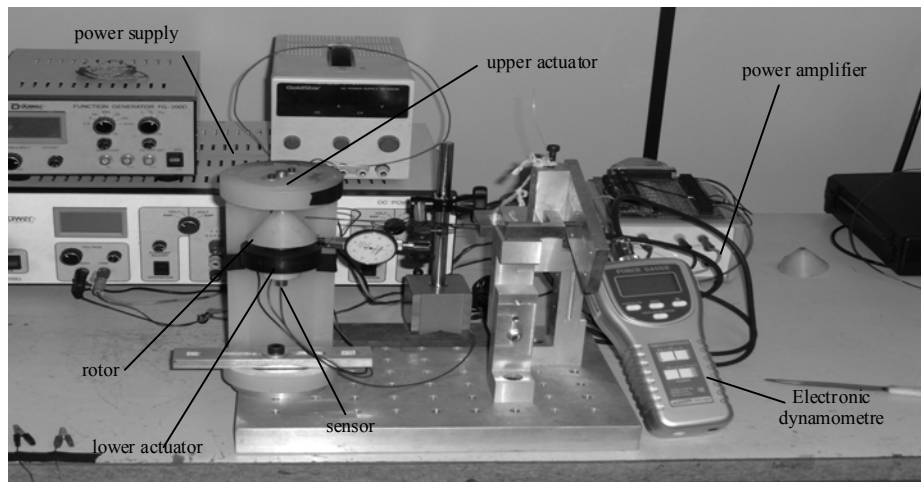


Figure 14. Magnetic bearing prototype for VAD experimental set up.

prototype and the experimental set up used to test it. A polymeric (Nylon) cylindrical structure supports, on its top side, a hybrid type electromagnet actuator, as depicted in Fig. 2c. (outer diameter of 25mm by 13mm height with 450 coil turns). In the lower side of the structure, a hybrid actuator and a non-contact eddy current, presented in Fig.3, are arranged (outer diameter 25mm by 17mm height and 450 coil turns). In the upper rotor end a cylindrical shape NdFeB magnet is placed (9mm diameter by 6mm height) and in its lower end an annular NdFeB magnet target is fixed (19mm diameter by 3,3mm height).

In the future, eight or more cylindrical shape NdFeB magnets (6mm diameter by 3mm height) will be arranged around de rotor lower perimeter, these magnets will be the cores of an electric DC brushless radial type motor that will drive the rotor, as shown

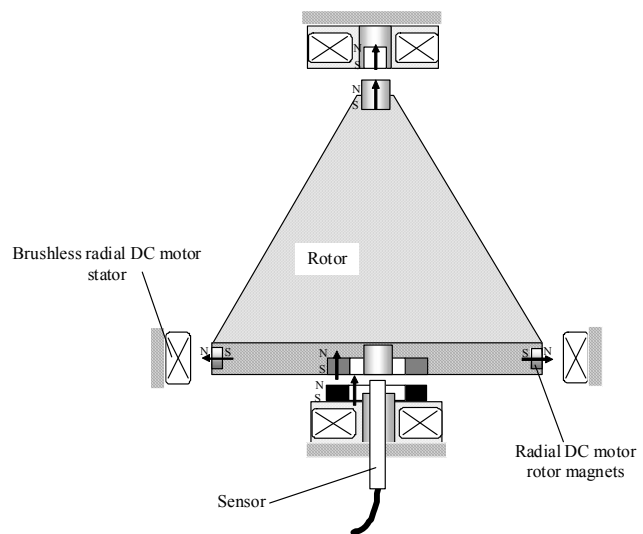


Figure 15. Future VAD-IDPC scheme with magnetic bearing suspension and the rotor driven by a brushless radial type DC motor.

in Fig.15. A conical shape rotor (Nylon, 50mm maximum by 10mm minimum diameters and by 43mm height) is set between the actuators and the sensor. As the objective here is only to test the magnetic bearing that will be applied to a truly VAD-IDPC prototype, no blades were machined in the rotor, no pump housing was constructed either and the rotor was driven by an air jet that acts tangential to its periphery. A computer is used to control the system according to a PID algorithm described by Eq. 5. Sensor signal is sampled to the computer through 12bits A/D converter and control signal is sent to the actuator through a 12bits D/A converter and a current amplifier, as shown by Fig. 13 control system block diagram.

Figure 16 shows the rotor being levitated by the developed magnetic bearing. As it is observed in the photo, a clearance (approximately 2mm) is maintained at the upper and the lower side of the rotor. The clearance between the sensor and the rotor is of approximately 1mm. Thus the rotor is suspended without any mechanical contact in a stable way. The sampling rate of the digital control executed by the computer, as well as the parameters of the PID controller, were adjusted by MATLAB[®] simulations and also experimentally. The optimization of such parameters will be treated in future work tasks. The objective here is to verify the stability and the stiffness of the suspension strategy. All bearing parameters are listed in table 1.

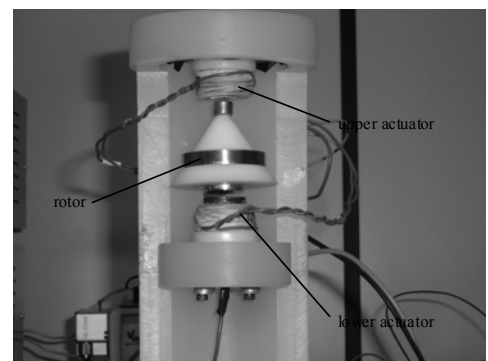


Figure 15. Rotor being levitated.

Table 1. System Parameters

Parameters	Symbols	Values	Units
Magnetic Constant	K_m	5000	N/m
Electromagnetic constant	K_t	1,65	N/A
Mass of rotor	m	$61.3 \cdot 10^{-3}$	kg
Inductance	L	5	mH
Resistance	R	12	Ω
Controller parameters			
Proportional gain	k	2	-
Derivative time	T_d	0.05	s
Integral time	T_i	20	s
Sampling rate	f	500	Hz

Figure 17 depicts rotor axial displacements with null rotation and spinning at 1200 rpm. Despite some axial oscillations, the rotor remains stable around the selected axial position for null and 1200 rpm rotations. The oscillations observed in this figure, when the rotor is with null rpm, are mainly due to electric noise and have maximum displacement of approximately 20 μm . On the other hand, when the rotor spins with 1200 rpm the maximum axial displacement is approximately 40 μm . This slight oscillations displacement increase is mainly due to rotor unbalanced forces in association with the electric noise. These results show the capability of the proposed actuator designs, see Figs. 2b and 3, and the controller in keeping the rotor stable in a precise axial position.

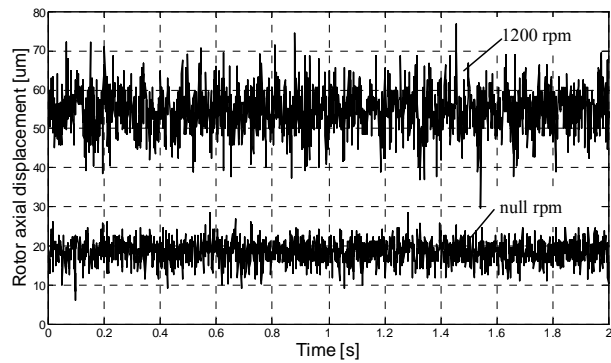


Figure 17. Rotor axial displacements with null rpm and 1200 rpm.

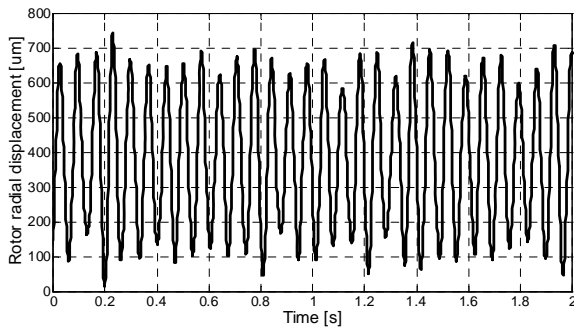


Figure 18. Rotor radial displacements response for 1200 rpm.

Figure 18 shows rotor radial displacement when it spins with 1200 rpm. Through this figure, one can see that the maximum rotor radial displacement measures approximately 0,7mm. Despite this large radial displacement, caused by the former mentioned rotor unbalanced forces, the rotor do not loose its radial passive stability, showing the capability of the proposed hybrid type actuators in maintaining the rotor spinning stable around its centered position. As observed in Fig. 18, the radial oscillations displacements remain steady; this is due to any radial damping force absences which are capable of attenuating these oscillations. In the future, this necessary radial damping force will be generated by the blood flowing between the rotor and the VAD's body.

The control system was also equipped with an input reference signal. So, a 75 μm step input was applied to the rotor axial position, the rotor axial step responses can be observed in Fig. 19. Through some overshooting, the rotor reaches the new commanded position in a short time and remains stable in this new position. This is another proof of the efficiency of the hybrid actuator and controller pair.

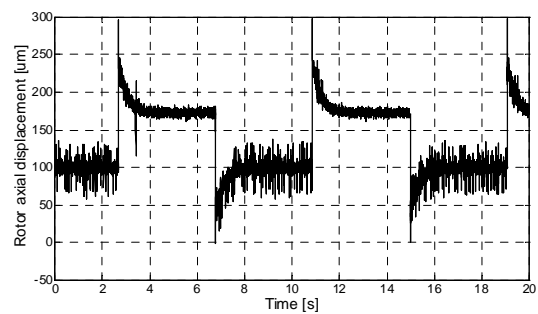


Figure 19. Step response for rotor axial direction.

Figure 20 presents the bearing radial force as a function of the rotor radial shift relative to its centre position and when the rotor is levitated. This figure shows that the radial stiffness is positive and measures approximately 490 N/mm, which assures rotor radial stability even for rotations greater than 1200rpm.

6. CONCLUSIONS

This report has presented some theoretical and experimental analyzes conducted in three hybrid type electromagnetic actuators, herein named upper actuators and the results done in a named lower hybrid actuator. The best actuator architecture of the three architectures analyzed has been the one that uses a mixed core. The strategy regarding application of a magnetic bearing

suspension to a centrifugal and implantable ventricular assist device, VAD, being jointly developed by Dante Pazzanese Cardiology Institute (IDPC) and by Escola Polit cnica of S o Paulo University, has also been discussed and tested. The magnetic bearing suspension, with active control only in one degree of freedom of the rotor, has as final objective the development of a VAD-IDPC for intra body use. The magnetic bearing suspension passive stiffness problems as well as the actuator design criterions were studied by numerical methods and experimentally. A prototype of the VAD with the magnetic bearing suspension has been constructed and tests demonstrate that a stable suspension of the rotor for rotations up to 1200 rpm has been reached and the rotor is also stable for some radial and axial disturbance forces applied to it. Future work tasks will treat the development of even more efficient actuators for the magnetic bearing, avoiding saturation problems of the actuator and of the current amplifier, thus allowing increase in the bearing passive stiffness, although considered satisfactory in the present work task, these passive stiffness can and need to be improved. Also a complete prototype of the VAD-IDPC with rotor blades, pump body, a brushless DC motor type to drive the rotor, as shown by Fig. 15, as well as tests conducted using animal blood will be the theme of future work tasks.

7. ACKNOWLEDGMENT

This research is sponsored by Funda o de Amparo   Pesquisa do Estado de S o Paulo, FAPESP.

8. REFERENCES

- Andrade, A., Biscegli, J., Dinkhuysen, J., Sousa, J.E., Ohashi, Y., Hemmings, S., Glueck, J., Kawahito, K. and Nose, Y. (1996), "Characteristics of a Blood Pump Combining the Centrifugal and Axial Pumping Principles: The Spiral Pump". *Artificial Organs*, Vol.20(6), 605-612.
- Astr m, H.J., H gglund, T., 1988, "Automatic tuning of PID controllers", Instrument society of America, 1988, 140 p.
- Don, B. O. (2000), "The History of Continuous-Flow Blood Pumps" *Artificial Organs*, Vol.24 (6), 401-404.
- Esmore, D., Kaye, D., Salomonsen, R., Buckland, M., Rowland, M., Negri, J., Rowley, Y., Woodard, J., Begg, J. and Ayre, P. (2005), "First clinical implant of the VentrAssist Left Ventricular Assist System as destination therapy for end-stage heart failure". *J Heart Lung Transplant*, Vol. 24 (8), 1150 – 1154.
- Hoshi, H., Katakoa, K., Ohuchi, K., Asama, J., Shinshi, T., Shimokohbe, A. and Takatani, S. (2005), "Magnetically Suspended Centrifugal Blood Pump With a Radial Magnetic Driver". *ASAIO Journal*, pp. 60-64.
- Fukamachi, K., Ochiai, Y., Doi, K., Massiello, A., Medvedev, A., Horvath, D., Gerhart, R., Chen, J., Krogulecki, A., Takagaki, M., Howard, M., Kopcak, M. and Golding, L.A.R.(2002) "Chronic Evaluation of the Cleveland Clinic CorAide Left Ventricular Assist System in Calves". *Artificial Organs*, Vol.26 (6), 529-533.
- Nojiri C. (2002), "Left ventricular assist system with a magnetically levitated impeller technology". *Nippon Geka Gakkai Zasshi*. Vol.103 (9), 607-617.
- Silva, I. and Horikawa, O. (2000), "An 1-dof Controlled Attraction Type Magnetic Bearing", *IEEE Transaction on Industry Applications*, Vol.36 (4), 1138.
- Westaby, S., Katsumata, T., Houlel, R, Evans, R. Pigott, D., Frazier, O. H. and Jarvik, R. (1998), "Jarvik2000 heart: Potential for Bridge to Myocyte Recovery". *Circulation*, Vol.98(15), 1568-74.
- Wieselthaler, G.M., Schima, H., Hiesmary, M., Pacher, R. Laufer, G., Noon, G.P. and DeBakey, M., Wolner, E. (2000), "First Clinical Experience with the DeBakey VAD Continuous-Axial-Flow Pump for Bridge to Transplantation", *Circulation*, Vol.101(4), 356-359.
- Yonnet, J.P. (1981), "Permanent Magnet Bearing and Coupling", *IEEE Trans.on Mag.*, Vol.17, 1169-1172.

9. RESPONSIBILITY NOTICE

The authors are the only responsible for the printed material included in this paper.

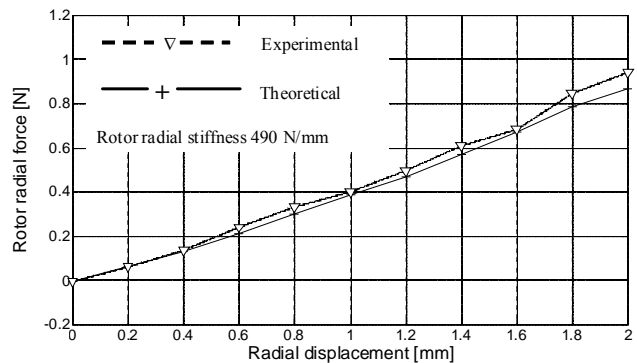


Figure 20. Levitated rotor radial force.